

# Self-organized Balanced Resources in Random Networks with Transportation Bandwidths

Chi Ho Yeung and K.Y. Michael Wong

Department of Physics, The Hong Kong University of Science and Technology,  
Hong Kong, China

**Abstract.** We apply statistical physics to study the task of resource allocation in random networks with limited bandwidths for the transportation of resources along the links. We derive algorithms which searches the optimal solution without the need of a global optimizer. For networks with uniformly high connectivity, the resource shortage of a node becomes a well-defined function of its capacity. An efficient profile of the allocated resources is found, with clusters of node interconnected by an extensive fraction of unsaturated links, enabling the resource shortages among the nodes to remain balanced. The capacity-shortage relation exhibits features similar to the Maxwell's construction. For scale-free networks, such an efficient profile is observed even for nodes of low connectivity.

**Keywords:** resource allocation, bandwidth, Maxwell's construction, scale-free networks, Bethe approximation, message-passing.

## 1 Introduction

Analytical techniques developed in statistical physics have been widely employed in the analysis of complex systems in a wide variety of fields, such as neural networks [1,2], econophysical models [3], and error-correcting codes [2,5]. Recently, a statistical physics perspective was successfully applied to the problem of resource allocation on sparse random networks [6,7]. Resource allocation is a well known network problem in the areas of computer science and operations management [8,9]. It is relevant to applications such as load balancing in computer networks, reducing Internet traffic congestion, and streamlining network flow of commodities [10,11].

In this paper, we analyze resource allocation on networks with finite bandwidths. We derive algorithms which enable us to find the optimal solutions without the need of a global optimizer. Compared with conventional techniques such as linear or quadratic programming [14], the adopted approach in this paper reduces the computational complexity. Furthermore, the analysis allows us to understand the underlying mechanisms during resource redistribution, on both scale-free and regular networks (i.e. networks with uniform connectivity). An efficient profile of the allocated resource is found with features similar to the Maxwell's construction.

## 2 The Model

We consider a network with  $N$  nodes, labelled  $i = 1, \dots, N$ . Each node  $i$  is randomly connected to  $c$  other nodes. The connectivity matrix is given by  $\mathcal{A}_{ij} = 1, 0$  for connected and unconnected node pairs respectively. We first develop a theory for sparse networks, namely, those of intensive connectivity  $c \sim O(1) \ll N$ , and subsequently consider its validity in networks of general connectivity, such as scale-free networks.

Each node  $i$  has a capacity  $\Lambda_i$  randomly drawn from a distribution  $\rho(\Lambda_i)$ . Positive and negative values of  $\Lambda_i$  correspond to supply and demand of resources respectively. The task of resource allocation involves transporting resources between nodes such that the demands of the nodes can be satisfied to the largest extent. Hence we assign  $y_{ij} \equiv -y_{ji}$  to be the *current* drawn from node  $j$  to  $i$ , aiming at reducing the *shortage*  $\xi_i$  of node  $i$  defined by

$$\xi_i = \max\left(-\Lambda_i - \sum_{(ij)} \mathcal{A}_{ij} y_{ij}, 0\right). \tag{1}$$

The magnitudes of the currents are bounded by the *bandwidth*  $W$ , i.e.,  $|y_{ij}| \leq W$ .

To minimize the shortage of resources after their allocation, we include in the total cost both the shortage cost and the transportation cost. Hence, the general cost function of the system can be written as

$$E = R \sum_{(ij)} \mathcal{A}_{ij} \phi(y_{ij}) + \sum_i \psi(\Lambda_i, \{y_{ij} | \mathcal{A}_{ij} = 1\}). \tag{2}$$

The summation  $(ij)$  corresponds to summation over all node pairs, and  $\Lambda_i$  is a quenched variable defined on node  $i$ .

In the present model of resource allocation, the first and second terms correspond to the transportation and shortage costs respectively. The parameter  $R$  corresponds to the *resistance* on the currents, and  $\Lambda_i$  is the capacity of node  $i$ . The transportation cost  $\phi(y_{ij})$  can be a general even function of  $y_{ij}$ . In this paper, we consider  $\phi$  and  $\psi$  to be concave functions of their arguments, that is,  $\phi'(y)$  and  $\psi'(\xi)$  are non-decreasing functions. Specifically, we have the quadratic transportation cost  $\phi(y) = y^2/2$ , and the quadratic shortage cost  $\psi(\Lambda_i, \{y_{ij} | \mathcal{A}_{ij} = 1\}) = \xi_i^2/2$ .

## 3 Analysis

The analysis of the model is made convenient by the introduction of the variables  $\xi_i$ . It can be written as the minimization of Eq. (2) in the space of  $y_{ij}$  and  $\xi_i$ , subject to the constraints

$$\Lambda_i + \sum_{(ij)} \mathcal{A}_{ij} y_{ij} + \xi_i \geq 0, \quad \xi_i \geq 0, \tag{3}$$

and the constraints on the bandwidths of the links  $|y_{ij}| \leq W$ .

Introducing Lagrange multipliers to the above inequality constraints with the Kuhn-Tucker condition, the function to be minimized becomes

$$L = \sum_i \left[ \psi(\xi_i) + \mu_i \left( \Lambda_i + \sum_{(ij)} \mathcal{A}_{ij} y_{ij} + \xi_i \right) + \alpha_i \xi_i \right] + \sum_{(ij)} \mathcal{A}_{ij} \left[ R\phi(y_{ij}) + \gamma_{ij}^+(W - y_{ij}) + \gamma_{ij}^-(W + y_{ij}) \right], \tag{4}$$

where  $\mu_i \leq 0$ ,  $\alpha_i \leq 0$ ,  $\gamma_{ij}^+ \leq 0$  and  $\gamma_{ij}^- \leq 0$ . Optimizing  $L$  with respect to  $y_{ij}$ , one obtains

$$y_{ij} = Y(\mu_j - \mu_i) \quad \text{with} \quad Y(x) = \max \left\{ -W, \min \left[ W, [\phi']^{-1} \left( \frac{x}{R} \right) \right] \right\}. \tag{5}$$

The Lagrange multiplier  $\mu_i$  is referred to as the *chemical potential* of node  $i$ , and  $\phi'$  is the derivative of  $\phi$  with respect to its argument. The function  $Y(\mu_j - \mu_i)$  relates the potential difference between nodes  $i$  and  $j$  to the current driven from node  $j$  to  $i$ . For the quadratic cost, it consists of a linear segment between  $\mu_j - \mu_i = \pm WR$  reminiscent of Ohm's law in electric circuits. Beyond this range,  $y$  is bounded above and below by  $\pm W$  respectively. Thus, obtaining the optimized configuration of currents  $y_{ij}$  among the nodes is equivalent to finding the corresponding set of chemical potentials  $\mu_i$ , from which the optimized  $y_{ij}$ 's are then derived from  $Y(\mu_j - \mu_i)$ . This implies that we can consider the original optimization problem in the space of chemical potentials.

We introduce the free energy at a temperature  $T \equiv \beta^{-1}$ ,

$$F = -T \ln Z, \tag{6}$$

where  $Z$  is the partition function

$$Z = \prod_{(ij)} \left( \int_{-W}^W dy_{ij} \right) \exp \left[ -\beta R \sum_{(ij)} \mathcal{A}_{ij} \phi(y_{ij}) - \beta \sum_i \psi(\Lambda_i, \{y_{ij} | \mathcal{A}_{ij} = 1\}) \right]. \tag{7}$$

The statistical mechanical analysis of the free energy can be carried out using the Bethe approximation, which is valid in the limit of low connectivity. In this approximation, a node is connected to  $c$  branches of the tree, and the correlations among the branches are neglected. In each branch, nodes are arranged in generations, A node is connected to an ancestor node of the previous generation, and another  $c - 1$  descendent nodes of the next generation.

We consider the vertex  $V(\mathbf{T})$  of a tree  $\mathbf{T}$ . We let  $F(y|\mathbf{T})$  be the free energy of the tree when a current  $y$  is drawn from the vertex by its ancestor node. One can express  $F(y|\mathbf{T})$  in terms of the free energies  $F(y_k|\mathbf{T}_k)$  of its descendents  $k = 1, \dots, c - 1$ ,

$$F(y|\mathbf{T}) = -T \ln \left\{ \prod_{k=1}^{c-1} \left( \int_{-W}^W dy_k \right) \exp \left[ -\beta \sum_{k=1}^{c-1} F(y_k|\mathbf{T}_k) - \beta R \sum_{k=1}^{c-1} \phi(y_k) - \beta \psi \left( \max(-\Lambda_{V(\mathbf{T})} - \sum_{k=1}^{c-1} y_k + y, 0) \right) \right] \right\}, \tag{8}$$

where  $\mathbf{T}_k$  represents the tree terminated at the  $k^{\text{th}}$  descendent of the vertex, and  $\Lambda_{V(\mathbf{T})}$  is the capacity of  $V(\mathbf{T})$ . We then consider the free energy as,

$$F(y|\mathbf{T}) = N_{\mathbf{T}} F_{\text{av}} + F_V(y|\mathbf{T}), \tag{9}$$

where  $N_{\mathbf{T}}$  is the number of nodes in the tree  $\mathbf{T}$ , and  $F_{\text{av}}$  is the vertex free energy per node.  $F_V(y|\mathbf{T})$  is referred to as the *vertex free energy*. Note that when a vertex is added to a tree, there is a change in the free energy due to the added vertex. In the language of the cavity method [4],  $F_V(y|\mathbf{T})$  are equivalent to the *cavity fields*, since they describe the state of the system when the ancestor node is absent. In the zero temperature limit, we obtain a recursion relation,

$$F_V(y|\mathbf{T}) = \min_{\{y_k || y_k| \leq W\}} \left[ \sum_{k=1}^{c-1} \left( F_V(y_k|\mathbf{T}_k) + R\phi(y_k) \right) + \psi \left( \max(-\Lambda_{V(\mathbf{T})} - \sum_{k=1}^{c-1} y_k + y, 0) \right) \right] - F_{\text{av}}. \tag{10}$$

$$F_{\text{av}}(y|\mathbf{T}) = \left\langle \min_{\{y_k || y_k| \leq W\}} \left[ \sum_{k=1}^c \left( F_V(y_k|\mathbf{T}_k) + R\phi(y_k) \right) + \psi \left( \max(-\Lambda_{V(\mathbf{T})} - \sum_{k=1}^c y_k, 0) \right) \right] \right\rangle_A. \tag{11}$$

### 4 Distributed Algorithms

A distributed algorithm can be obtained by iterating the chemical potentials of the nodes. The optimal currents are given by Eq. (5) in terms of the chemical potentials  $\mu_i$  which, from Eqs. (1) and (4), are related to their neighbors via

$$\mu_i = \begin{cases} 0 & \text{for } h_i^{-1}(0) > 0, \\ h_i^{-1}(0) & \text{for } -\psi'(0) \leq h_i^{-1}(0) \leq 0, \\ g_i^{-1}(0) & \text{for } h_i^{-1}(0) < -\psi'(0), \end{cases} \tag{12}$$

where  $h_i(x)$  and  $g_i(x)$  are given by

$$h_i(x) = -\Lambda_i - \sum_j \mathcal{A}_{ij} Y(\mu_j - x), \quad g_i(x) = \psi' \circ h_i(x) + x, \tag{13}$$

with function  $Y$  again given Eq. (5).  $h_i(x)$  is the shortage of resource at node  $i$  when  $\mu_i$  takes the value  $x$ .  $\psi' \circ h_i(x)$  is then the corresponding dissatisfaction cost per unit resource of node  $j$ . This provides a simple local iteration method for the optimization problem in which the optimal currents can be evaluated from the potential differences of neighboring nodes.

An alternative algorithm can be obtained by adopting message-passing approaches, which have been successful in problems such as error-correcting codes [12] and probabilistic inference [13]. However, in contrast to other message-passing algorithms which pass conditional probability estimates of discrete variables to neighboring nodes, the messages in the present context are more complex, since they are free energy functions  $F_V(y|\mathbf{T})$  of the continuous variable  $y$ . Inspired by the success of replacing the function messages by their first and second derivatives in [7], we follow the same route and form two-parameter messages. Let  $(A_{ij}, B_{ij}) \equiv (\partial F_V(y_{ij}|\mathbf{T}_j)/\partial y_{ij}, \partial^2 F_V(y_{ij}|\mathbf{T}_j)/\partial y_{ij}^2)$ . These are the messages passed from node  $j$  to its ancestor node  $i$ , based on the messages received from its descendents in the tree  $\mathbf{T}_j$ . To obtain recursion relation of the messages, we minimize in the space of the current adjustments  $\epsilon_{jk}$  the vertex free energy

$$F_{ij} = \sum_{k \neq i} \mathcal{A}_{jk} \left[ A_{jk} \epsilon_{jk} + \frac{1}{2} B_{jk} \epsilon_{jk}^2 + R \phi'_{jk} \epsilon_{jk} + \frac{R}{2} \phi''_{jk} \epsilon_{jk}^2 \right] + \psi(\xi_j), \quad (14)$$

subject to the constraints

$$\sum_{k \neq i} \mathcal{A}_{jk} (y_{jk} + \epsilon_{jk}) - y_{ij} + A_j + \xi_j \geq 0, \quad \xi_j \geq 0, \quad (15)$$

together with the constraints on bandwidths  $|y_{jk} + \epsilon_{jk}| \leq W$ .  $\phi'_{jk}$  and  $\phi''_{jk}$  represent the first and second derivatives of  $\phi(y)$  at  $y = y_{jk}$  respectively. We introduce Lagrange multiplier  $\mu_{ij}$  for constraints (15). After optimizing the energy function of node  $j$ , the messages from node  $j$  to  $i$  are given by

$$\begin{aligned}
 A_{ij} &\leftarrow -\mu_{ij}, & (16) \\
 B_{ij} &\leftarrow \begin{cases} 0 & \text{for } h_{ij}^{-1}(0) > 0, \\ \left\{ \sum_{k \neq i} \mathcal{A}_{jk} (R \phi''_{jk} + B_{jk})^{-1} \right. \\ \quad \times \Theta \left[ W - \left| y_{jk} - \frac{R \phi'_{jk} + A_{jk} + \mu_{ij}}{R \phi''_{jk} + B_{jk}} \right| \right] \Big\}^{-1} & \text{for } -\psi'(0) \leq h_{ij}^{-1}(0) \leq 0, \\ \left\{ \psi''(\xi)^{-1} + \sum_{k \neq i} \mathcal{A}_{jk} (R \phi''_{jk} + B_{jk})^{-1} \right. \\ \quad \times \Theta \left[ W - \left| y_{jk} - \frac{R \phi'_{jk} + A_{jk} + \mu_{ij}}{R \phi''_{jk} + B_{jk}} \right| \right] \Big\}^{-1} & \text{for } h_{ij}^{-1}(0) < -\psi'(0), \end{cases} & (17)
 \end{aligned}$$

where

$$g_{ij}(x) = [\psi' \circ h_{ij}](x) + x, \tag{18}$$

$$\mu_{ij} = \begin{cases} 0 & \text{for } h_{ij}^{-1}(0) > 0, \\ h_{ij}^{-1}(0) & \text{for } -\psi'(0) \leq h_{ij}^{-1}(0) \leq 0, \\ g_{ij}^{-1}(0) & \text{for } h_{ij}^{-1}(0) < -\psi'(0), \end{cases} \tag{19}$$

and  $h_{ij}(x)$  is defined by

$$h_{ij}(x) = y_{ij} - A_j - \sum_{k \neq i} \max \left\{ -W, \min \left[ W, y_{jk} - \frac{R\phi'_{jk} + A_{jk} + x}{R\phi''_{jk} + B_{jk}} \right] \right\}. \tag{20}$$

Since the messages are simplified to be the first two derivatives of the vertex free energies, it is essential for the nodes to determine the *working points* at which the derivatives are taken. Optimal currents  $y_{jk}$  are thus computed and sent backward from node  $j$  to the descendent nodes  $k \neq i$ . These backward messages serve as a key in information provision to descendents, so that the derivatives in the subsequent messages are to be taken at the updated working points. Minimizing the free energy (14) with respect to  $y_{jk}$ , the backward message is found to be

$$y_{jk} \leftarrow \max \left\{ -W, \min \left[ W, y_{jk} - \frac{R\phi'_{jk} + A_{jk} + \mu_{ij}}{R\phi''_{jk} + B_{jk}} \right] \right\}. \tag{21}$$

An important result of our study is that for the frictionless case with  $\psi'(0) = 0$ , the message-passing algorithm, in the two-parameter approximation, yield solutions *identical* to the previous algorithm, *which is exact* for all connectivities, as long as the algorithms converges. This is a remarkable result since the message-passing algorithm is originally derived for dilute networks only.

## 5 The High Connectivity Limit

We consider the case that the bandwidth of individual links scales as  $\tilde{W}/c$  when the connectivity increases, where  $\tilde{W}$  is a constant. Thus the total bandwidth  $\tilde{W}$  available to an individual node remains a constant.

We start by writing the chemical potentials using Eq. (12),

$$\mu_i = \min \left[ A_i + \sum_{j=1}^N \mathcal{A}_{ij} Y(\mu_j - \mu_i), 0 \right]. \tag{22}$$

In the high connectivity limit, the interaction of a node with all its connected neighbors become self-averaging, making it a function which is singly dependent on its own chemical potential, namely,

$$\sum_{j=1}^N \mathcal{A}_{ij} Y(\mu_j - \mu_i) \approx cM(\mu_i). \quad (23)$$

Physically, the function  $M(\mu)$  corresponds to the average interaction of a node with its neighbors when its chemical potential is  $\mu$ . Thus, we can write Eq. (22) as

$$\mu = \min[\Lambda + cM(\mu), 0], \quad (24)$$

where  $\mu$  is now a function of  $\Lambda$ , and we have

$$M(\mu_i) = \int_{-\infty}^{\infty} d\Lambda \rho(\Lambda) Y(\mu(\Lambda) - \mu_i) \quad (25)$$

where we have written the chemical potential of the neighbors as  $\mu(\Lambda)$ , assuming that they are well-defined functions of their capacities  $\Lambda$ .

To explicitly derive  $M(\mu)$ , we take advantage of the fact that the rescaled bandwidth,  $\tilde{W}/c$  vanishes in the high connectivity limit, so that the current function  $Y(\mu_j - \mu_i)$  is effectively a sign function, which implies that the current on a link is always saturated. (This approximation is not fully valid if  $c$  is large but finite and will be further refined in subsequent discussions) Thus, we approximate

$$M(\mu_i) = \frac{\tilde{W}}{c} \int_{-\infty}^{\infty} d\Lambda \rho(\Lambda) \text{sgn}[\mu(\Lambda) - \mu_i]. \quad (26)$$

Assuming that  $\mu(\Lambda)$  is a monotonic function of  $\Lambda$ , and for Gaussian distribution of capacities,  $\mu(\Lambda)$  is explicitly given by

$$\mu = \min \left[ \Lambda - \tilde{W} \text{erf} \left( \frac{\Lambda - \langle \Lambda \rangle}{\sqrt{2}} \right), 0 \right]. \quad (27)$$

This equation relates the chemical potential of a node, i.e. the shortage after resource allocation, to its initial resource before. Resource allocation through a large number of links results in a well-defined function relating the two quantities.

Eq. (27) gives a well-defined function  $\mu(\Lambda)$  as long as  $\tilde{W} \leq \sqrt{\pi/2}$ . However, when  $\tilde{W} > \sqrt{\pi/2}$ , turning points exist in  $\mu(\Lambda)$  as shown in Fig. 1(a). This creates a thermodynamically unstable scenario, since in the region of  $\mu(\Lambda)$  with negative slope, nodes with lower capacities have higher chemical potentials than their neighbors with higher capacities. Mathematically, the non-monotonicity of  $\mu(\Lambda)$  means that  $\text{sgn}[\mu(\Lambda) - \mu_i]$  and  $\text{sgn}(\Lambda - \Lambda_i)$  are no longer necessarily equal, and Eq. (27) is no longer valid.

Nevertheless, Eq. (22) permits another solution of constant  $\mu$  in a range of  $\Lambda$ . Hence, we propose that the unstable region of  $\mu(\Lambda)$  should be replaced by a range of constant  $\mu$  as shown in Fig. 1(b) analogous to Maxwell's construction in thermodynamics.

In the high connectivity limit, resources are so efficiently allocated that the resources of the rich nodes are maximally allocated to the poor nodes. By

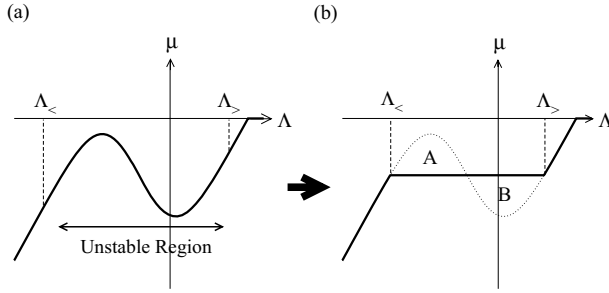


Fig. 1. Maxwell's construction on  $\mu(\Lambda)$

considering the conservation of resources, and letting  $(\Lambda_<, \mu_o)$  and  $(\Lambda_>, \mu_o)$  be the end points of the Maxwell's construction as shown in Fig. 1(b). we arrive at

$$\begin{aligned}
 & - \int_{\Lambda_<}^{\Lambda_>} d\Lambda \rho(\Lambda) \mu_o - \left( \int_{\Lambda_>}^{\Lambda_o} + \int_{-\infty}^{\Lambda_<} \right) d\Lambda \rho(\Lambda) \mu(\Lambda) \\
 & = - \int_{-\infty}^{\Lambda_o} d\Lambda \rho(\Lambda) \Lambda - \Lambda_o \int_{\Lambda_o}^{\infty} d\Lambda \rho(\Lambda).
 \end{aligned} \tag{28}$$

where  $\Lambda_o$  is given by  $\Lambda_o = \tilde{W} \int_{-\infty}^{\Lambda_o} d\Lambda \rho(\Lambda)$ . Nodes with  $\Lambda \geq \Lambda_o$  send out their resources without drawing inward currents from their neighbors, and can be regarded as *donors*. Substituting Eqs. (24), (25) in the range  $\Lambda < \Lambda_<$  and  $\Lambda > \Lambda_>$ , we arrive at the condition

$$\mu_o \int_{\Lambda_<}^{\Lambda_>} d\Lambda \rho(\Lambda) = \int_{\Lambda_<}^{\Lambda_>} d\Lambda \rho(\Lambda) \mu(\Lambda), \tag{29}$$

which implies that the value of  $\mu_o$  should be chosen such that the areas A and B in Fig. 1(b), weighted by the distribution  $\rho(\Lambda)$ , should be equal.

For capacity distributions  $\rho(\Lambda)$  symmetric with respect to  $\langle \Lambda \rangle$ , we have  $\mu_o = \langle \Lambda \rangle = (\Lambda_< + \Lambda_>)/2$ . As a result, the function  $\mu(\Lambda)$  is given by

$$\mu(\Lambda) = \begin{cases} \langle \Lambda \rangle & \text{for } \mu_< < \mu < \mu_>, \\ \min \left[ \Lambda - \tilde{W} \operatorname{erf} \left( \frac{\Lambda - \langle \Lambda \rangle}{\sqrt{2}} \right), 0 \right] & \text{otherwise,} \end{cases} \tag{30}$$

where as  $\Lambda_<$  and  $\Lambda_>$  are respectively given by the lesser and greater roots of the equation  $x = \langle \Lambda \rangle + \tilde{W} \operatorname{erf}[(x - \langle \Lambda \rangle)/\sqrt{2}]$ .

Nodes  $i$  with chemical potentials  $\mu_i = \langle \Lambda \rangle$  represent clusters of nodes interconnected by an extensive fraction of unsaturated links, which provides the freedom to fine tune their currents so that the shortages among the nodes are



uniform. They will be referred to as the *balanced nodes*. The fraction  $f_{\text{bal}}$  of balanced nodes is given by the equation

$$f_{\text{bal}} = \text{erf}\left(\frac{\tilde{W} f_{\text{bal}}}{\sqrt{2}}\right). \tag{31}$$

Note that  $f_{\text{bal}}$  has the same dependence on  $\tilde{W}$  for all negative  $\langle \Lambda \rangle$ . The inset of Fig. 4 shows that when the total bandwidth  $\tilde{W}$  increases beyond  $\sqrt{\pi/2}$ , the fraction of balanced nodes increases, reflecting the more efficient resource allocation brought by the convenience of increased bandwidths. When  $\tilde{W}$  becomes very large, a uniform chemical potential of  $\langle \Lambda \rangle$  networkwide is recovered, converging to the case of non-vanishing bandwidths.

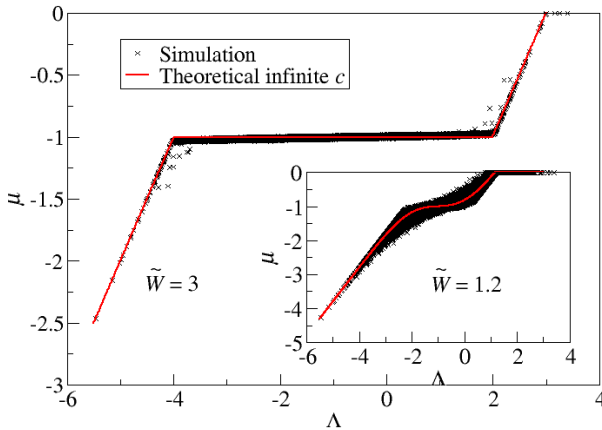


**Fig. 2.** The simulation results of  $\mu(\Lambda)$  for  $N = 10000$ ,  $c = 15$ ,  $R = 0.1$ ,  $\langle \Lambda \rangle = -1$  and  $\tilde{W} = 3$  with 70000 data points, compared with theoretical prediction. Inset: The corresponding results for  $\tilde{W} = 1.2$ .

We compare the analytical result of  $\mu(\Lambda)$  in Eq. (30) with simulations in Fig. 2. For  $\tilde{W} > \sqrt{\pi/2}$ , data points  $(\Lambda, \mu)$  of individual nodes from network simulations follow the analytical result of  $\mu(\Lambda)$ , giving an almost perfect overlap of data. The presence of the balanced nodes with effectively constant chemical potentials is obvious and essential to explain the behavior of the majority of data points from simulations. On the other hand, for  $\tilde{W} < \sqrt{\pi/2}$ , the analytical  $\mu(\Lambda)$  shows no turning point as shown in the inset of Fig. 2. Despite the scattering of data points, they generally follow the trend of the theoretical  $\mu(\Lambda)$ .

Our analysis can be generalized to the case of large but finite connectivity, where the approximation in Eq. (26) is not fully valid. This modifies the chemical potentials of the balanced nodes, for which Eq. (26) has to be replaced by

$$M(\mu) = \frac{\tilde{W}}{c} \left[ \int_{\Lambda_>}^{\infty} d\Lambda \rho(\Lambda) - \int_{-\infty}^{\Lambda_<} d\Lambda \rho(\Lambda) \right] + \int_{\Lambda_<}^{\Lambda_>} d\Lambda \rho(\Lambda) \left( \frac{\mu(\Lambda) - \mu}{R} \right). \tag{32}$$

We introduce an ansatz of a linear relationship between  $\mu$  and  $\Lambda$  for the balanced nodes, namely,

$$\mu = m\Lambda + b. \tag{33}$$

After direct substitution of Eq. (33) into  $M(\mu)$  given by Eq. (32), we get the self-consistent equations for  $m$  and  $b$ ,

$$m = \frac{R}{R + c \operatorname{erf}\left(\frac{\Lambda - \langle \Lambda \rangle}{\sqrt{2}}\right)}, \quad b = \frac{c \operatorname{erf}\left(\frac{\Lambda - \langle \Lambda \rangle}{\sqrt{2}}\right)}{R + c \operatorname{erf}\left(\frac{\Lambda - \langle \Lambda \rangle}{\sqrt{2}}\right)} \langle \Lambda \rangle. \tag{34}$$

Thus, the Maxwell’s construction has a non-zero slope when the connectivity is finite.

We remark that the approximation in Eq. (32) assumes that the potential differences of the balanced nodes lie in the range of  $2R\tilde{W}/c$ , so that their connecting links remain unsaturated. Note that the end points of the Maxwell’s construction have chemical potentials  $\langle \Lambda \rangle \pm R\tilde{W}/c$  respectively, rendering the approximation in Eq. (32) *exact* at one special point, namely, the central point of the Maxwell’s construction. Hence, this approximation works well in the central region of the Maxwell’s construction, while deviations are expected near the end points.

In the simulation data shown in Fig. 3, the data points of  $(\Lambda, \mu)$  from different ratios of  $R/c$  follow the trend of the corresponding analytical results, both within and outside the linear region, with increasing scattering within the linear region as  $R/c$  increases. As expected, there are derivations between the analytical and simulational results at the two ends of the linear region, with smoothed corners appearing in the simulation data, especially in the case of  $R/c = 2/20$ .

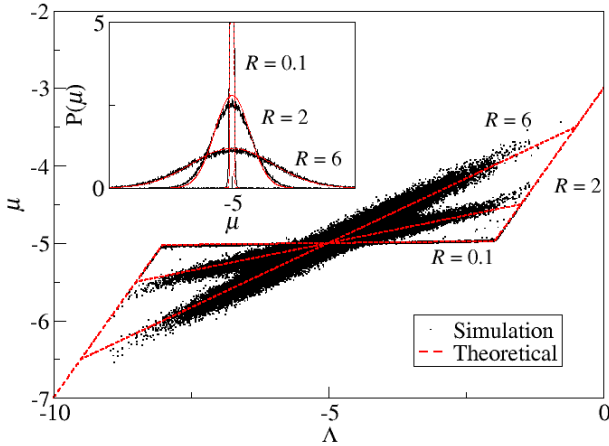


**Fig. 3.** Simulation results of  $(\Lambda, \mu)$  for  $N = 2 \times 10^5$ ,  $\tilde{W} = 3$ ,  $c = 12$  and  $\langle \Lambda \rangle = -5$  at different values of  $R$ , each with 65000 data points. as compared to the theoretical predictions. Inset: the corresponding chemical potential distribution  $P(\mu)$  of the 3 cases.

We note that when  $R/c$  increases, the gradient of the linear region increases, corresponding to a less uniform allocation of resources.

Remarkably, as evident from Eq. (34), even with constant available bandwidth  $\tilde{W}$ , increasing connectivity causes  $m$  to decrease, and hence sharpens the chemical potential distribution. The narrower distributions correspond to higher efficiency in resource allocation. It leads us to realize the potential benefits of increasing connectivity in network optimization even for a given constant total bandwidth connecting a node.

## 6 Scale-Free Networks

We have considered the allocation of resources in regular networks in the high connectivity limit. However, recent studies of complex networks show that many realistic communication networks have highly heterogeneous structure, and the connectivity distribution obeys a power law [15]. These networks, commonly known as scale-free networks, are characterized by the presence of hubs, which are nodes with very high connectivities, and are found to modify the network behavior significantly. Hence, it is interesting to study the allocation of resources in scale-free networks.

The simulation results are presented in Fig. 4, where we plot the data points of  $(\Lambda, \mu)$  from nodes of  $c = 3$  in scale-free networks. Despite their low connectivity, their capacity-shortage relation exhibit the flat distribution characteristic of the Maxwell’s construction, coinciding with the analytical results of the high connectivity limit. This shows that the presence of hubs in scale-free networks increases the global efficiency of resource allocation, leading to a more uniform distribution of resources.

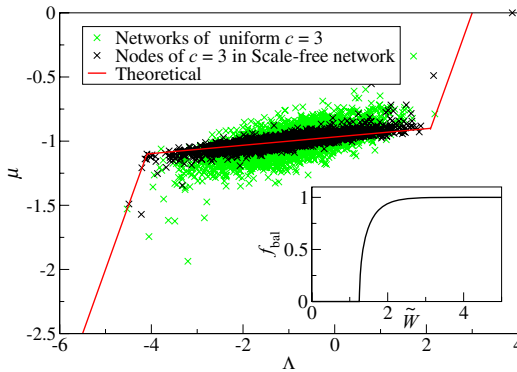


**Fig. 4.** Simulation results of  $(\Lambda, \mu)$  for networks of  $N = 2 \times 10^5$ ,  $\tilde{W} = 3$ ,  $R = 0.1$  and  $\langle \Lambda \rangle = -1$  with (a) uniform connectivity of  $c = 3$  and (b) scale-free network of  $P(c) \sim c^{-3}$  with  $c \geq 3$ . each with 2500 data points. as compared to the theoretical predictions Eq. (34). Inset: the dependence of the  $f_{\text{bal}}$  in Eq. (31) on the bandwidth  $\tilde{W}$ .

To confirm this advantage of the scale-free topology, we also plot in the figure the data points obtained from networks of uniform connectivity  $c = 3$ . Evidently, the data points are much more scattered away from the Maxwell's construction.

## 7 Conclusion

We have applied statistical mechanics to study an optimization task of resource allocation on a network, in which nodes with different capacities are connected by links of finite bandwidths. By adopting suitable cost functions, such as quadratic transportation and shortage costs, the model can be applied to the study of realistic networks. We employ the Bethe approximation to derive recursive relations of the vertex free energies, which are useful in both algorithmic and analytic aspects.

In particular, the study reveals interesting effects due to finite bandwidths. A remarkable phenomenon is found in networks with fixed total bandwidths per node, where bandwidths per link vanish in the high connectivity limit. For sufficiently large total bandwidths, clusters of balanced nodes self-organized to have a uniform shortage reminiscent of the Maxwell's construction in thermodynamics. In scale-free networks, such clusters even include nodes with low connectivity, implying a more efficient resource allocation compared to networks with uniform connectivity. We believe that the techniques presented in this paper are useful in many different network optimization problems and will lead to a large variety of potential applications.

## Acknowledgements

We thank David Saad for very meaningful discussions. This work is supported by the Research Grant Council of Hong Kong (grant numbers HKUST 603606, HKUST 603607 and HKUST 604008).

## References

1. Hertz, J., Krogh, A., Palmer, R.G.: Introduction to the Theory of Neural Computation. Addison-Wesley, Redwood City (1991)
2. Nishimori, H.: Statistical Physics of Spin Glasses and Information Processing. Oxford University Press, Oxford (2001)
3. Challet, D., Marsili, M., Zhang, Y.-C.: Minority Games. Oxford University Press, Oxford (2005)
4. Mézard, M., Parissi, G., Virasoro, M.A.: Spin Glass Theory and Beyond. World Scientific, Singapore (1987)
5. Kabashima, Y., Saad, D.: J. Phys. A 37, R1 (2004)
6. Wong, K.Y.M., Saad, D.: Phys. Rev. E 74, 010104 (2006)
7. Wong, K.Y.M., Saad, D.: Phys. Rev. E 76, 011115 (2007)

8. Peterson, L., Davie, B.S.: Computer Networks: A Systems Approach. Academic Press, San Diego (2000)
9. Ho, Y.C., Servi, L., Suri, R.: Large Scale Syst. 1, 51 (1980)
10. Shenker, S., Clark, D., Estrin, D., Herzog, S.: Comput. Commun. Rev. 26, 19 (1996)
11. Rardin, R.L.: Optimization in Operations Research. Prentice Hall, Englewood Cliffs (1998)
12. Opper, M., Saad, D. (eds.): Advanced Mean Field Methods. MIT Press, Cambridge (1999)
13. Mackey, D.J.C.: Information Theory, Inference and Learning Algorithms. Cambridge University Press, Cambridge (2003)
14. Bertsekas, D.: Linear Network Optimization. MIT Press, Cambridge (1991)
15. Barabási, A.L., Albert, R.: Science 286, 509 (1999)